Published OnlineFirst May 2, 2012; DOI:10.1158/0008-5472.CAN-12-0299

Overexpression of CD44s promotes the expression of vimentin and tumor invasiveness of hepatocellular carcinoma cells, whereas the knockdown of CD44s attenuates these changes

To investigate whether CD44s regulates the mesenchymal phenotype of HCC cells, we transiently transfected PLC/PRF/5 cells with a human CD44s expression vector. The overexpression of CD44s increased the expression of vimentin but did not decrease the expression of E-cadherin (Fig. 2A and B). Furthermore, the overexpression of CD44s increased the *in vitro* invasion of the transfected cells by 7-fold (Fig. 2C). Next, we examined the effect of the siRNA knockdown of CD44 in HLF cells, which normally have high CD44 expression, to determine whether CD44s is essential for the expression of vimentin in HCC cells. CD44 siRNA attenuated the expression of vimentin at the mRNA and protein levels (Fig. 2D and E). Furthermore, in HLF cells pretreated with CD44 siRNA, the addition of a CD44s expression vector reversibly increased the expression of vimentin (Fig. 2E). The results from an *in vitro* invasion assay revealed that HLF cells transfected with CD44 siRNA exhibited a decrease in invasion compared with cells transfected with a control siRNA (Fig. 2F). We observed similar results in high CD44s expressing HLE and SK HEP-1 cells (Supplementary Fig. S2). Overexpression of CD44s in PLC/PRF/5 cells did not decrease the expression of E-cadherin. Moreover, we could not detect the upregulation of E-cadherin in the CD44 knockdown cells. These results suggested that CD44s regulates the expression of vimentin and tumor cell invasion in HCC cells.

CD44s is induced by TGF-β and regulates the TGF-β–mediated mesenchymal phenotype in hepatocellular carcinoma cells

TGF-β signaling is central to tumorigenesis and tumor progression because it regulates many critical cellular processes, including cell proliferation, EMT, and stem cell maintenance (32). HLF and HLE cells express detectable levels of phosphorylated Smad2, and the expression of E-cadherin was increased after incubation with a TGFβ type I receptor kinase inhibitor in HLF and HLE cells, suggesting that TGF-β signaling plays a crucial role in EMT in HCC cells (33). TGF-β1 is overexpressed in tumor cells, and this overexpression correlates with a poor prognosis in patients with HCC (34, 35). Thus, we investigated the role of CD44 in TGF-β signaling. We screened the activation status of TGF-β signaling by measuring phosphorylated Smad2 (phospho-Smad2) expression in the 5 HCC cell lines. As reported previously, HLF and HLE cells expressed detectable levels of phosphorylated Smad2 whereas SK HEP-1 cells did not (Fig. 3A). The precise mechanism of CD44 expression in SK HEP-1 cells with low phospho-Smad2 expression is unclear from our study. SK HEP-1 cells are originally derived from endothelial cells, which express CD44

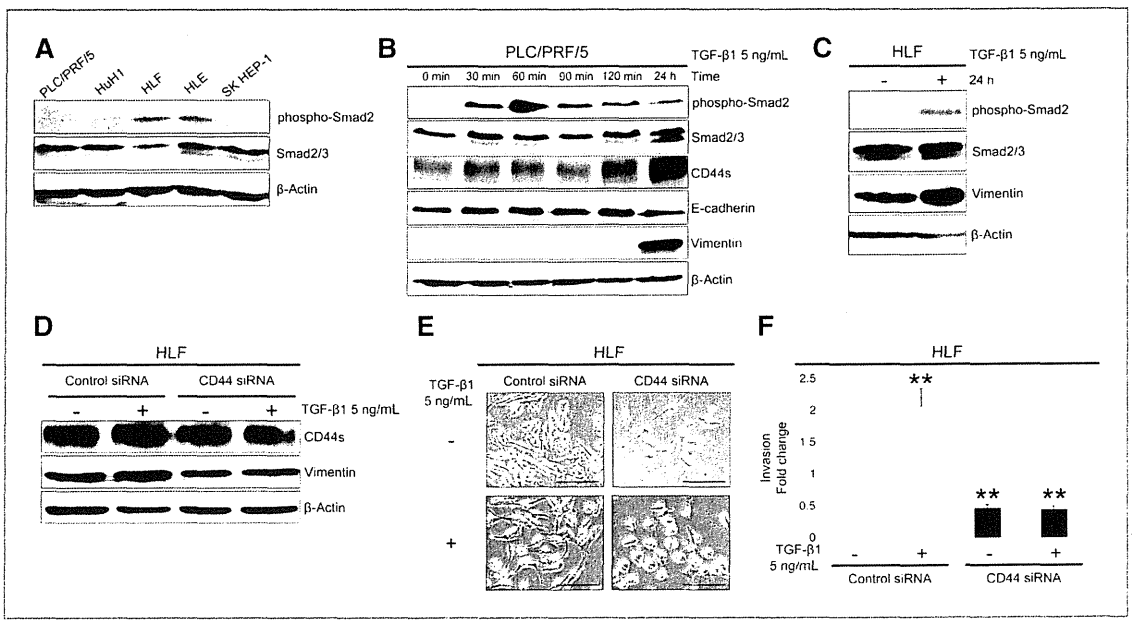

CD44s is induced by TGF-β1 and regulates the TGF-β–mediated mesenchymal phenotype in hepatocellular carcinoma cells. A, the expression of phosphorylated Smad2 (phospho-Smad2) in the 5 HCC cell lines, as determined by Western blot analysis. B, immunoblot analysis of phospho-Smad2 and the expression levels of CD44s, E-cadherin, and vimentin following TGF-β1 (5 ng/mL) treatment in PLC/PRF/5 cells. C, immunoblot analysis of phospho-Smad2 and the expression level of vimentin following TGF-β1 (5 ng/mL) treatment in HLF cells. D, immunoblot analysis of the expression levels of CD44s and vimentin with or without TGF-β1 (5 ng/mL) treatment for 24 hours in HLF cells transfected with siRNA targeted against CD44 compared with control cells. E, phase-contrast images with or without TGF-β1 (5 ng/mL) treatment for 24 hours in the HLF cells transfected with siRNA targeted against CD44 compared with control cells. Scale bars, 200 μm. F, the invasive capacity of HLF cells with or without TGF-β1 (5 ng/mL) treatment for 24 hours after transfection with siRNA targeted against CD44 compared with untreated control cells. The data represent the means ± SD ($n = 3$; **, $P < 0.01$).

Published OnlineFirst May 2, 2012; DOI:10.1158/0008-5472.CAN-12-0299

(36, 37). In human endothelial cells, other growth factors, such as basic fibroblast growth factor, VEGF, and hepatocyte growth factor/scatter factor (HGF/SF), can induce the expression of CD44 (37, 38). Therefore, an alternative mechanism may be associated with the expression of CD44 in SK HEP-1 cells. We next examined the role of CD44 in the TGF-β–mediated mesenchymal phenotype of HCC cells. Treatment with TGF-β1 induced a mesenchymal spindle-like morphology in PLC/PRF/5 cells (Supplementary Fig. S3A). Following treatment with TGF-β1 (5 ng/mL), phospho-Smad2 expression in PLC/PRF/5 cells progressively increased in a time-dependent manner and peaked after 60 minutes (Fig. 3B). The downregulation of E-cadherin, the upregulation of vimentin, and the expression of CD44s were induced after 24 hours of treatment with TGF-β1 in PLC/PRF/5 cells (Fig. 3B). The expression of E-cadherin mRNA was decreased after 6 hours and restored after 24 hours (Supplementary Fig. S3B). The expression of vimentin and CD44 mRNA were elevated after 24 hours. Several transcription factors, including Snail, Slug, and Twist1 promote EMT in epithelial cells (4). The expression of Snail mRNA was increased after treatment with TGF-β1 and peaked after 3 hours (Supplementary Fig. S3C). The expression of Slug was not affected, and no expression of Twist1 in response to TGF-β1 was detected in PLC/PRF/5 cells. These results suggested that TGF-β signaling triggered the mesenchymal phenotype and induced the expression of CD44s in HCC cells. Next, we examined the effects of CD44s on the TGF-β–mediated mesenchymal phenotype. HLF cells also displayed progressively increased phospho-Smad2 levels in a time-dependent manner following incubation with TGF-β1 (5 ng/mL), and the levels peaked after 60 minutes (Supplementary Fig. S3D). In addition, upregulation of vimentin was induced by TGF-β1 after 24 hours

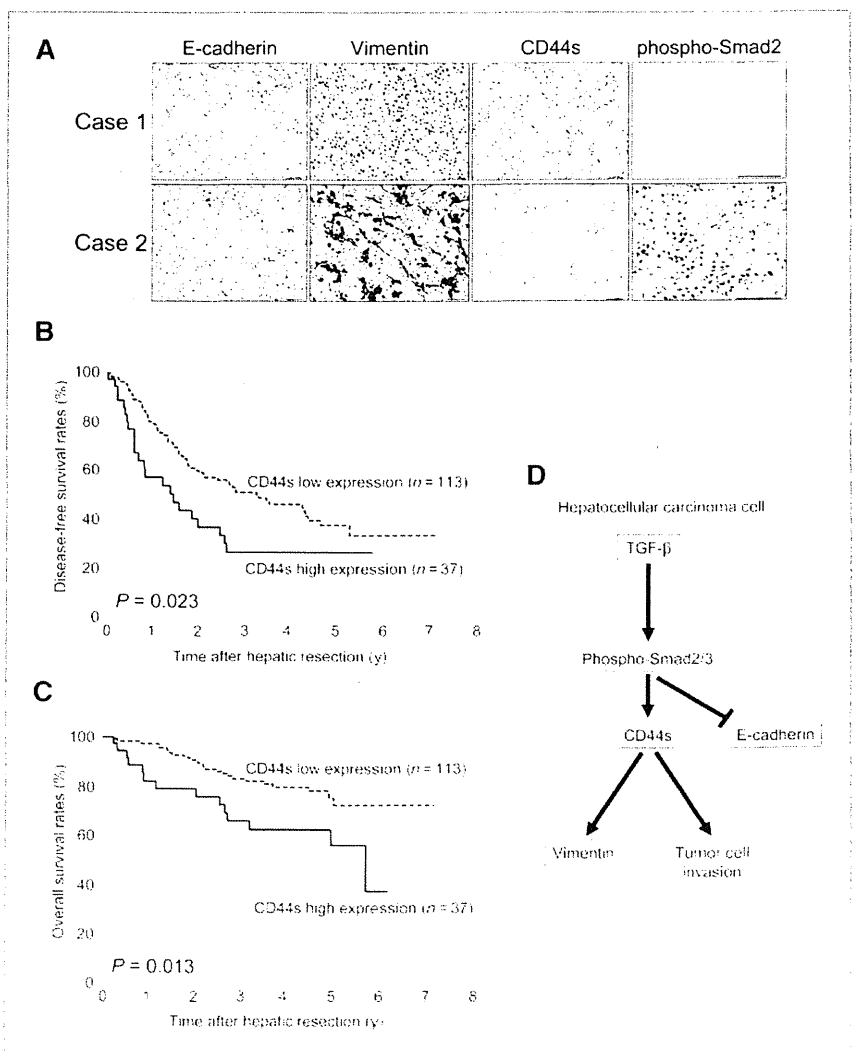

Figure 4. CD44s expression is associated with E-cadherin and vimentin expression and poor prognosis in patients with hepatocellular carcinoma. A, immunohistochemical staining of E-cadherin, vimentin, CD44s, and phospho-Smad2 in representative cases with low CD44s expression (case 1) and high CD44s expression (case 2). Scale bars, 50 μm. B, Kaplan–Meier survival analysis of disease-free survival in 150 HCC patients comparing the high CD44s expression group and the low CD44s expression group using the log-rank test. C, Kaplan–Meier survival analysis of overall survival in 150 HCC patients comparing the high CD44s expression group and the low CD44s expression group using the log-rank test. D, model of the regulation of the mesenchymal phenotype by CD44s in hepatocellular carcinoma cells following the induction of CD44s expression by TGF-β signaling. Subsequently, CD44s promotes vimentin expression and tumor cell invasion. The expression of E-cadherin may be suppressed by other mechanisms in the TGF-β signaling pathway.

Published OnlineFirst May 2, 2012; DOI:10.1158/0008-5472.CAN-12-0299

Table 1. [illegible]

	E-cadherin			Vimentin			phospho-Smad2 nuclear positivity		
	Low ($n = 92$)	High ($n = 58$)	P^a	Low ($n = 126$)	High ($n = 24$)	P^a	Low ($n = 123$)	High ($n = 27$)	P^a
CD44s									
Low ($n = 113$)	64	49	0.039	108	5	<0.001	106	7	<0.001
High ($n = 37$)	28	9		18	19		17	20	

Abbreviations: CD44s, CD44 standard isoform; phospho-Smad2, phosphorylated Smad2.
[a]Estimated by χ^2 test.

of treatment in HLF cells (Fig. 3C). These results indicated that TGF-β signaling enhances the expression of vimentin in HLF cells. CD44 siRNA inhibited the TGF-β–mediated vimentin expression, mesenchymal spindle-like morphology, and tumor invasiveness in HLF cells (Fig. 3D–F). These results suggested that CD44s is essential for the TGF-β–mediated mesenchymal phenotype in HCC cells.

CD44s expression is associated with E-cadherin and vimentin expression and poor prognosis in patients with hepatocellular carcinoma

To confirm the *in vitro* finding that the TGF-β–mediated mesenchymal phenotype and induction of CD44s are correlated in HCC cells, we analyzed the expression levels of CD44s, E-cadherin, vimentin, and phospho-Smad2 by IHC in 150 HCC patient samples. High expression of CD44s (e.g., case 2 shown in Fig. 4A) was detected in 25% (37 of 150) of the samples, and low E-cadherin expression was significantly associated with high vimentin expression ($P = 0.001$). High CD44s expression was significantly associated with low E-cadherin expression ($P = 0.039$), high vimentin expression ($P < 0.001$), and high phospho-Smad2 nuclear positivity ($P < 0.001$; Table 1). These data suggested that the activation of TGF-β signaling induces CD44s expression and a mesenchymal phenotype in patients with HCC. With regard to clinicopathologic factors, a significant correlation was shown between high CD44s expression and large tumor size ($P = 0.003$), multiple tumors ($P = 0.032$), and poor tumor differentiation ($P = 0.020$; Table 2). We further investigated the association between the expression levels of CD44s, vimentin, and E-cadherin and the clinicopathologic factors in HCC patients. In a subgroup of patients with a CD44s^{high}/vimentin^{high}/E-cadherin^{low} expression profile, the

Table 2. Correlation between CD44s expression and the clinicopathologic factors of 150 HCC patients

	CD44s high expression ($n = 37$)	CD44s low expression ($n = 113$)	P
Age: <60/>60 (y)	9/28	35/78	0.441
Sex: Male/Female	30/7	93/20	0.867
HBs-Ag: Negative/Positive	28/9	79/34	0.501
HCV-Ab: Negative/Positive	20/17	61/52	0.994
Child–Pugh classification: A/B	32/5	103/10	0.412
AFP: <20/>20 (ng/mL)	16/21	60/53	0.298
PIVKA-II: ≤107/>107 (mAU/mL)	18/19	57/56	0.850
Tumor size: <3/>3 (cm)	5/32	45/68	**0.003**
Tumor number: 1/2≤	21/16	85/28	**0.032**
Tumor encapsulation: Absent/present	2/35	15/98	0.190
Tumor differentiation: Moderate, well/poor	25/12	96/17	**0.020**
LCSGJ TNM Stage: 1,2/3, 4	18/19	71/42	0.127
AJCC/UICC TNM Stage: 1,2/3, 4	28/9	94/19	0.309
Vascular invasion: Absent/present	30/7	102/11	0.136

NOTE: Vascular invasion, portal vein (3rd branch, 2nd branch, 1st branch, or trunk) or hepatic vein (trunk of hepatic vein or IVC) invasion were defined via macroscopic examination of the resected specimens.
Abbreviations: CD44s, CD44 standard isoform; HBs-Ag, hepatitis B surface antigen; HCV-Ab, hepatitis C antibody; AFP, α-fetoprotein; PIVKA II, protein-induced vitamin K absence-II; LCSGJ, Liver Cancer Study Group of Japan.

Published OnlineFirst May 2, 2012; DOI:10.1158/0008-5472.CAN-12-0299

incidence of vascular invasion was significantly higher than that in a subgroup of patients with a CD44s^{low}/vimentin^{low}/E-cadherin^{high} expression profile (25% vs. 0%, respectively, $P < 0.001$; Supplementary Table S1). In all 150 HCC patients studied, high CD44s expression was more associated with frequent vascular invasion than low CD44s expression was, but this correlation did not reach a statistically significant difference (19% vs. 10%, $P = 0.136$). These results suggested that not only the mesenchymal phenotype via CD44s but also the loss of E-cadherin expression plays an important role of the vascular invasion in HCC patients. Notably, high CD44s expression was significantly associated with shorter disease-free survival ($P = 0.023$; Fig. 4B) and shorter overall survival ($P = 0.013$; Fig. 4C).

Discussion

In this study, CD44s, but not the variant isoforms, regulates the mesenchymal phenotype in HCC cells. In patients with HCC, tumoral CD44s overexpression was associated with the mesenchymal phenotype, as characterized by low E-cadherin expression and high vimentin expression. Interestingly, CD44s mRNA was the dominant form of CD44 mRNA present in human HCC cell lines, whereas the presence of high levels of the CD44v have been proposed as an important metastatic tumor marker in a number of cancers such as colon and lung cancer (39, 40). In breast cancer, CD44s was essential for the response to TGF-β during EMT, and the gain of CD44s expression was accompanied by a loss of expression of the variant isoforms (41). These findings suggest that the dominant form of CD44 isoforms in different tumors varies according to the location of the cancer cells.

TGF-β primes cancer cells for pulmonary metastasis and metastatic colonization of cancer cells in bones (42, 43). A recent study showed that TGF-β in the blood activates TGF-β signaling in cancer cells, resulting in their transition to an invasive mesenchymal-like phenotype with enhanced metastatic potential (44). Furthermore, a link between TGF-β and the CD44^{high} population has been described in breast cancer and glioblastoma. TGF-β increases the CD44^{high}/CD24^{low} population, which is enriched in CSCs, through the induction of EMT in breast cancer (8). In addition, glioma-initiating cells (GIC) expressed high levels of CD44, and the inhibition of TGF-β signaling decreased the GIC population in glioblastomas (45). These results agree with our studies showing a novel role for CD44s in the TGF-β–mediated mesenchymal phenotype in HCC cells.

Although TGF-β signaling can induce the mesenchymal phenotype as characterized by low E-cadherin expression and high vimentin expression in epithelial cells, the mediators between TGF-β signaling and the mesenchymal phenotype are still unclear. This study suggests that CD44 plays a downstream role in TGF-β signaling by regulating the expression of vimentin and tumor cell invasiveness, and that CD44 does not affect the expression of E-cadherin, which may be suppressed by other mechanisms involved in the TGF-β pathway (Fig. 4D). The expression of Snail was elevated after 3 hours, and the expression of E-cadherin was suppressed after 6 hours. The induction of Snail expression in response to TGF-β is mediated by Smad2/3. Smad3 binds to the *Snail* promoter and activates its transcription (46). Smad3/4 and Snail interact to form a transcriptional repressor complex, which targets the promoter of E-cadherin (47). The time course of the activation of TGF-β signaling and the expression of Snail and E-cadherin in this study suggested that TGF-β signaling may suppress the expression of E-cadherin via Snail in HCC cells.

We showed that high CD44s expression was a poor prognostic factor following curative hepatic resection of primary HCC. In addition to CD44s, several other variant isoforms (CD44v5, CD44v6, CD44v7-8, and CD44v10) correlate with a worse prognosis in HCC patients, as determined by immunohistochemical analysis (26). Our investigations about clinicopathologic factors showed a significant correlation between CD44s expression and large tumor size, multiple tumors, and poor tumor differentiation in patients with HCC. Consistent with our *in vitro* analysis, high CD44s expression correlated with high vimentin expression in human HCC cells. Furthermore, in patients with HCC, we showed that phospho-Smad2 nuclear positivity was associated with high CD44s expression and that a CD44s^{high}/vimentin^{high}/E-cadherin^{low} expression profile was associated with vascular invasion. Together with our *in vitro* studies, these results suggested that the TGF-β–CD44s axis plays an important role in the vascular invasion of HCC. TGF-β signaling was recently determined to maintain the stem cell–like properties of tumor-initiating cells (32). Chaffer and Weinberg suggested a new concept of cancer cell metastasis in which cancer cells traveling through the circulation system are considered to be CSCs because of their anchorage-independent survival and the fact that these CSCs extravasate and invade into the parenchyma at distant organs (48). These observations support our findings that CD44s, a CSC marker, plays a downstream role in TGF-β signaling in HCC cells. We are continuing our studies to examine whether CD44s has an important role in the modulation of CSC properties in HCC cells.

In conclusion, our study suggests that the standard isoform of CD44, a CSC marker, regulates the TGF-β–mediated mesenchymal phenotype, and that its expression indicates poor prognosis in patients with HCC. This information will be valuable for a better understanding of the relationship between CSCs and the mesenchymal phenotype induced by EMT; in addition, our results establish CD44s as a novel therapeutic target for HCC.

Disclosure of Potential Conflicts of Interest

No potential conflicts of interest were disclosed.

Authors' Contributions

Conception and design: K. Mima, H. Okabe, T. Ishimoto
Development of methodology: K. Mima, H. Okabe, H. Baba
Acquisition of data (provided animals, acquired and managed patients, provided facilities, etc.): H. Okabe, S. Nakagawa, H. Kuroki, O. Nagano, H. Baba
Analysis and interpretation of data (e.g., statistical analysis, biostatistics, computational analysis): K. Mima, H. Okabe, H. Hayashi, H. Kuroki, M. Watanabe, H. Baba
Writing, review, and/or revision of the manuscript: K. Mima, H. Okabe, H. Hayashi, T. Beppu, H. Baba

Published OnlineFirst May 2, 2012; DOI:10.1158/0008-5472.CAN-12-0299

Administrative, technical, or material support (i.e., reporting or organizing data, constructing databases): H. Okabe, S. Nakagawa, M. Tamada
Study supervision: K. Mima, H. Okabe, M. Watanabe, H. Saya

Acknowledgments

The authors thank Keisuke Miyake and Naoko Yokoyama for their valuable technical assistance and also Eri Takahashi for her useful suggestions.

The costs of publication of this article were defrayed in part by the payment of page charges. This article must therefore be hereby marked *advertisement* in accordance with 18 U.S.C. Section 1734 solely to indicate this fact.

Received January 30, 2012; revised April 7, 2012; accepted April 25, 2012; published OnlineFirst May 2, 2012.

References

1. El-Serag HB. Hepatocellular carcinoma. N Engl J Med 2011;365:1118–27.
2. Poon RT, Ng IO, Fan ST, Lai EC, Lo CM, Liu CL, et al. Clinicopathologic features of long-term survivors and disease-free survivors after resection of hepatocellular carcinoma: a study of a prospective cohort. J Clin Oncol 2001;19:3037–44.
3. Polyak K, Weinberg RA. Transitions between epithelial and mesenchymal states: acquisition of malignant and stem cell traits. Nat Rev Cancer 2009;9:265–73.
4. Thiery JP, Acloque H, Huang RY, Nieto MA. Epithelial-mesenchymal transitions in development and disease. Cell 2009;139:871–90.
5. Yang MH, Chen CL, Chau GY, Chiou SH, Su CW, Chou TY, et al. Comprehensive analysis of the independent effect of twist and snail in promoting metastasis of hepatocellular carcinoma. Hepatology 2009;50:1464–74.
6. Lee TK, Poon RT, Yuen AP, Ling MT, Kwok WK, Wang XH, et al. Twist overexpression correlates with hepatocellular carcinoma metastasis through induction of epithelial-mesenchymal transition. Clin Cancer Res 2006;12:5369–76.
7. Chen L, Chan TH, Yuan YF, Hu L, Huang J, Ma S, et al. CHD1L promotes hepatocellular carcinoma progression and metastasis in mice and is associated with these processes in human patients. J Clin Invest 2010;120:1178–91.
8. Mani SA, Guo W, Liao MJ, Eaton EN, Ayyanan A, Zhou AY, et al. The epithelial-mesenchymal transition generates cells with properties of stem cells. Cell 2008;133:704–15.
9. Ponta H, Sherman L, Herrlich PA. CD44: from adhesion molecules to signalling regulators. Nat Rev Mol Cell Biol 2003;4:33–45.
10. Zoller M. CD44: can a cancer-initiating cell profit from an abundantly expressed molecule? Nat Rev Cancer 2011;11:254–67.
11. Clevers H. The cancer stem cell: premises, promises and challenges. Nat Med 2011;17:313–9.
12. Yang ZF, Ho DW, Ng MN, Lau CK, Yu WC, Ngai P, et al. Significance of CD90 + cancer stem cells in human liver cancer. Cancer Cell 2008;13:153–66.
13. Al-Hajj M, Wicha MS, Benito-Hernandez A, Morrison SJ, Clarke MF. Prospective identification of tumorigenic breast cancer cells. Proc Natl Acad Sci U S A 2003;100:3983–8.
14. Dalerba P, Dylla SJ, Park IK, Liu R, Wang X, Cho RW, et al. Phenotypic characterization of human colorectal cancer stem cells. Proc Natl Acad Sci U S A 2007;104:10158–63.
15. Prince ME, Sivanandan R, Kaczorowski A, Wolf GT, Kaplan MJ, Dalerba P, et al. Identification of a subpopulation of cells with cancer stem cell properties in head and neck squamous cell carcinoma. Proc Natl Acad Sci U S A 2007;104:973–8.
16. Li C, Heidt DG, Dalerba P, Burant CF, Zhang L, Adsay V, et al. Identification of pancreatic cancer stem cells. Cancer Res 2007;67:1030–7.
17. Scheel C, Eaton EN, Li SH, Chaffer CL, Reinhardt F, Kah KJ, et al. Paracrine and autocrine signals induce and maintain mesenchymal and stem cell states in the breast. Cell 2011;145:926–40.
18. Ishimoto T, Nagano O, Yae T, Tamada M, Motohara T, Oshima H, et al. CD44 variant regulates redox status in cancer cells by stabilizing the xCT subunit of system xc(-) and thereby promotes tumor growth. Cancer Cell 2011;19:387–400.
19. Hiyoshi Y, Kamohara H, Karashima R, Sato N, Imamura Y, Nagai Y, et al. MicroRNA-21 regulates the proliferation and invasion in esophageal squamous cell carcinoma. Clin Cancer Res 2009;15:1915–22.
20. Okabe H, Beppu T, Hayashi H, Ishiko T, Masuda T, Otao R, et al. Hepatic stellate cells accelerate the malignant behavior of cholangiocarcinoma cells. Ann Surg Oncol 2011;18:1175–84.
21. Livak KJ, Schmittgen TD. Analysis of relative gene expression data using real-time quantitative PCR and the 2(-Delta Delta C(T)) Method. Methods 2001;25:402–8.
22. Japan LCSGJ. The general rules for the clinical and pathological study of primary liver cancer. 5th ed., revised version. Tokyo: Kanehara; 2009.
23. Minagawa M, Ikai I, Matsuyama Y, Yamaoka Y, Makuuchi M. Staging of hepatocellular carcinoma: assessment of the Japanese TNM and AJCC/UICC TNM systems in a cohort of 13,772 patients in Japan. Ann Surg 2007;245:909–22.
24. Vauthey JN, Lauwers GY, Esnaola NF, Do KA, Belghiti J, Mirza N, et al. Simplified staging for hepatocellular carcinoma. J Clin Oncol 2002;20:1527–36.
25. Yang MH, Hsu DS, Wang HW, Wang HJ, Lan HY, Yang WH, et al. Bmi1 is essential in Twist1-induced epithelial-mesenchymal transition. Nat Cell Biol 2010;12:982–92.
26. Endo K, Terada T. Protein expression of CD44 (standard and variant isoforms) in hepatocellular carcinoma: relationships with tumor grade, clinicopathologic parameters, p53 expression, and patient survival. J Hepatol 2000;32:78–84.
27. Ishimoto T, Oshima H, Oshima M, Kai K, Torii R, Masuko T, et al. CD44 + slow-cycling tumor cell expansion is triggered by cooperative actions of Wnt and prostaglandin E2 in gastric tumorigenesis. Cancer Sci 2010;101:673–8.
28. Chiba T, Miyagi S, Saraya A, Aoki R, Seki A, Morita Y, et al. The polycomb gene product BMI1 contributes to the maintenance of tumor-initiating side population cells in hepatocellular carcinoma. Cancer Res 2008;68:7742–9.
29. Yamashita T, Ji J, Budhu A, Forgues M, Yang W, Wang HY, et al. EpCAM-positive hepatocellular carcinoma cells are tumor-initiating cells with stem/progenitor cell features. Gastroenterology 2009;136:1012–24.
30. Ma S, Chan KW, Hu L, Lee TK, Wo JY, Ng IO, et al. Identification and characterization of tumorigenic liver cancer stem/progenitor cells. Gastroenterology 2007;132:2542–56.
31. Haraguchi N, Ishii H, Mimori K, Tanaka F, Ohkuma M, Kim HM, et al. CD13 is a therapeutic target in human liver cancer stem cells. J Clin Invest 2010;120:3326–39.
32. Ikushima H, Miyazono K. TGFbeta signalling: a complex web in cancer progression. Nat Rev Cancer 2010;10:415–24.
33. Fransvea E, Angelotti U, Antonaci S, Giannelli G. Blocking transforming growth factor-beta up-regulates E-cadherin and reduces migration and invasion of hepatocellular carcinoma cells. Hepatology 2008;47:1557–66.
34. Bedossa P, Peltier E, Terris B, Franco D, Poynard T. Transforming growth factor-beta 1 (TGF-beta 1) and TGF-beta 1 receptors in normal, cirrhotic, and neoplastic human livers. Hepatology 1995;21:760–6.
35. Abou-Shady M, Baer HU, Friess H, Berberat P, Zimmermann A, Graber H, et al. Transforming growth factor betas and their signaling receptors in human hepatocellular carcinoma. Am J Surg 1999;177:209–15.
36. Heffelfinger SC, Hawkins HH, Barrish J, Taylor L, Darlington GJ. SK HEP-1: a human cell line of endothelial origin. In Vitro Cell Dev Biol 1992;28A:136–42.
37. Griffioen AW, Coenen MJ, Damen CA, Hellwig SM, van Weering DH, Vooys W, et al. CD44 is involved in tumor angiogenesis; an activation antigen on human endothelial cells. Blood 1997;90:1150–9.
38. Hiscox S, Jiang WG. Regulation of endothelial CD44 expression and endothelium-tumour cell interactions by hepatocyte growth factor/scatter factor. Biochem Biophys Res Commun 1997;233:1–5.

Published OnlineFirst May 2, 2012; DOI:10.1158/0008-5472.CAN-12-0299

39. Kuniyasu H, Oue N, Tsutsumi M, Tahara E, Yasui W. Heparan sulfate enhances invasion by human colon carcinoma cell lines through expression of CD44 variant exon 3. Clin Cancer Res 2001;7:4067–72.
40. Miyoshi T, Kondo K, Hino N, Uyama T, Monden Y. The expression of the CD44 variant exon 6 is associated with lymph node metastasis in non-small cell lung cancer. Clin Cancer Res 1997;3:1289–97.
41. Brown RL, Reinke LM, Damerow MS, Perez D, Chodosh LA, Yang J, et al. CD44 splice isoform switching in human and mouse epithelium is essential for epithelial-mesenchymal transition and breast cancer progression. J Clin Invest 2011;121:1064–74.
42. Padua D, Zhang XH, Wang Q, Nadal C, Gerald WL, Gomis RR, et al. TGFbeta primes breast tumors for lung metastasis seeding through angiopoietin-like 4. Cell 2008;133:66–77.
43. Yin JJ, Selander K, Chirgwin JM, Dallas M, Grubbs BG, Wieser R, et al. TGF-beta signaling blockade inhibits PTHrP secretion by breast cancer cells and bone metastases development. J Clin Invest 1999;103:197–206.
44. Labelle M, Begum S, Hynes RO. Direct signaling between platelets and cancer cells induces an epithelial-mesenchymal-like transition and promotes metastasis. Cancer Cell 2011;20:576–90.
45. Anido J, Saez-Borderias A, Gonzalez-Junca A, Rodon L, Folch G, Carmona MA, et al. TGF-beta receptor inhibitors target the CD44(high)/Id1(high) glioma-initiating cell population in human glioblastoma. Cancer Cell 2010;18:655–68.
46. Hoot KE, Lighthall J, Han G, Lu SL, Li A, Ju W, et al. Keratinocyte-specific Smad2 ablation results in increased epithelial-mesenchymal transition during skin cancer formation and progression. J Clin Invest 2008;118:2722–32.
47. Vincent T, Neve EP, Johnson JR, Kukalev A, Rojo F, Albanell J, et al. A SNAIL1-SMAD3/4 transcriptional repressor complex promotes TGF-beta mediated epithelial-mesenchymal transition. Nat Cell Biol 2009;11:943–50.
48. Chaffer CL, Weinberg RA. A perspective on cancer cell metastasis. Science 2011;331:1559–64.

Original article

External biliary drainage and liver regeneration after major hepatectomy

R. Otao[1], T. Beppu[1,2], T. Isiko[1], K. Mima[1], H. Okabe[1], H. Hayashi[1], T. Masuda[1], A. Chikamoto[1], H. Takamori[1] and H. Baba[1]

[1]Department of Gastroenterological Surgery, Graduate School of Medical Sciences, Kumamoto University, and [2]Department of Multidisciplinary Treatment for Gastroenterological Cancer, Innovation Centre for Translational Research, Kumamoto University Hospital, Kumamoto, Japan
Correspondence to: Professor H. Baba, Department of Gastroenterological Surgery, Graduate School of Medical Sciences, Kumamoto University, 1-1-1 Honjo, Kumamoto 860-8556, Japan (e-mail: hdobaba@kumamoto-u.ac.jp)

Background: Bile acid signalling and farnesoid X receptor activation are assumed to be essential for liver regeneration. This study was designed to investigate the association between serum bile acid levels and extent of liver regeneration after major hepatectomy.

Methods: Patients who underwent left- or right-sided hemihepatectomy between 2006 and 2009 at the authors' institution were eligible for inclusion. Patients were divided into two groups: those undergoing hemihepatectomy with external bile drainage by cystic duct tube (group 1) and those having hemihepatectomy without drainage (group 2). Serum bile acid levels were measured before and after hepatectomy. Computed tomography was used to calculate liver volume before hepatectomy and remnant liver volume on day 7 after surgery.

Results: A total of 46 patients were enrolled. Mean(s.d.) serum bile acid levels on day 3 after hemihepatectomy were significantly higher in group 2 than in group 1 (11·6(13·5) *versus* 2·7(2·1) μmol/l; $P = 0·003$). Regenerated liver volumes on day 7 after hepatectomy were significantly greater in group 2 138·1(135·9) ml *versus* 40·0(158·8) ml in group 1; $P = 0·038$). Liver regeneration volumes and rates on day 7 after hemihepatectomy were positively associated with serum bile acid levels on day 3 after hemihepatectomy ($P = 0·006$ and $P < 0·001$ respectively). The incidence of bile leakage was similar in the two groups.

Conclusion: Initial liver regeneration after major hepatectomy was less after biliary drainage and was associated with serum bile acid levels. External biliary drainage should be used judiciously after liver resection.

Paper accepted 29 June 2012
Published online in Wiley Online Library (www.bjs.co.uk). **DOI:** 10.1002/bjs.8906

Introduction

Hepatic resection is one of the most effective treatments for patients with liver tumours[1]. However, major hepatectomy is associated with high rates of morbidity and mortality because of deterioration of liver function. In Japan, most patients with hepatocellular carcinoma have relatively poor hepatic functional reserve owing to chronic liver disorders such as hepatitis B or C infection[2]. In this context, sufficient liver regeneration after major hepatectomy is important to prevent postoperative liver failure.

Previous experimental animal studies have revealed that bile acid signalling and farnesoid X receptor (FXR) activation are essential for early liver regeneration[3–5]. FXR belongs to the nuclear receptor superfamily and is highly expressed in liver and intestine. Increased serum bile acid levels accelerate, whereas decreased levels inhibit, liver regeneration after partial hepatectomy[3]. Preoperative external biliary drainage compared with internal biliary drainage leads to loss of bile acid and results in delayed liver regeneration after partial hepatectomy in rats[6–8].

Bile acid signalling has previously been demonstrated to be essential for liver regeneration after portal vein embolization (PVE) in humans[9]. However, limited data are available regarding the involvement of bile acid signalling in liver regeneration after partial hepatectomy in humans. This study investigated the association between external

biliary drainage and extent of liver regeneration after major hepatectomy in humans.

Methods

All patients undergoing right or left hepatectomy between July 2006 and December 2009 at the Department of Gastroenterological Surgery, Graduate School of Medical Sciences, Kumamoto University, were eligible for inclusion in the study, which was conducted as a retrospective analysis of a prospectively collected database. Only patients who underwent (extended) hemihepatectomy were selected to avoid the effects of small or complex resections on liver regeneration. Patients with previous PVE, other combined operative procedures, macroscopic portal vein tumour thrombus, or insufficient perioperative data or diagnostic images were excluded. Selected patients were classified into two groups according to the surgical procedure performed. Group 1 consisted of patients who underwent hemihepatectomy with external bile drainage by a cystic duct tube (C tube) to reduce the rate of postoperative biliary leakage[10]. Group 2 comprised patients who had hemihepatectomy without external bile drainage. Written informed consent was obtained from all study participants. The study protocol conformed to the ethical guidelines of the 1975 Declaration of Helsinki and was approved by the institutional review committee.

Hemihepatectomy was performed in a systematic manner in all patients. Patients with preoperative biliary drainage, previous cholecystectomy, bile duct excision or Child–Pugh grade B disease were excluded. During the study, the use of C-tube drainage was not absolutely required. Patients with no bile leakage from the cutting surface and no bile duct injury were mainly assigned to the no C-tube drainage group. The chief surgeon decided whether to use the C tube.

In all patients, serum bile acid levels were measured before, and 1, 3, 7 and 14 days after hemihepatectomy. Serum samples were collected early in the morning after overnight fasting. Oral intake was permitted from the day after hepatic resection. Serum bile acid levels, indocyanine green retention rate at 15 min and total bilirubin levels were measured using a liquid-stable enzymatic colorimetric assay, fluorescence assay and 2,5-dichlorophenyldiazonium assay respectively. Liver transection was performed by an ultrasonic surgical aspirator with precoagulation technique and liver hanging manoeuvre[10]. The number of Pringle manoeuvres applied (15 min of clamping and 5 min of release) was kept to a minimum. The amount of blood loss was calculated from blood in suction devices and gauze weight. The Child–Pugh classification was used to assess liver function.

Liver volumetry

Computed tomography (CT) was performed in all patients within 7 days before surgery and at 7 days after hepatectomy. For volumetric analysis, axial images of the portal venous phase of contrast-enhanced CT and volumetry software, AZE VirtualPlace® (AZE, Chiyoda-ku, Tokyo, Japan), was used. The weight of the resected specimen was measured immediately after surgery on a balance. The density of the resected liver was considered to be approximately 1·0 g/ml[11]. The numerical value of volume of the resected specimen is normally approximately equal to the weight; therefore, volume was defined to be equal to weight. Remnant liver volume estimated immediately after hepatectomy was defined as the difference between the volume before hepatectomy and resected liver weight. The following volume parameters were defined: volume A (V_A), total liver volume before hepatectomy measured by CT volumetry; volume B (V_B), volume of the resected specimen; and volume C (V_C), liver volume calculated by CT volumetry on day 7 after hepatectomy. Regenerated liver volume was calculated as $V_C - (V_A - V_B)$ and percentage liver regeneration was calculated as 100 per cent $\times [V_C - (V_A - V_B)]/(V_A - V_B)$.

Statistical analysis

Baseline data are presented as mean(s.d.). Data for the different groups and categorical data were compared using unpaired *t* tests and χ^2 test respectively. The unpaired two-group *t* test was used to evaluate changes in remnant liver volume after hepatectomy. Pearson's correlation was used to perform simple linear regression to study the association between increases in liver regeneration volumes and rates and serum bile acid levels. All significance tests were two-sided, and $P < 0{\cdot}050$ was considered to be statistically significant. The statistical software package SPSS® Statistics for Windows® version 18·0·0 (IBM, Chicago, Illinois, USA) was used for statistical analysis.

Results

A total of 409 partial hepatectomies were performed at the authors' institution during the study period. Seventy-nine consecutive patients underwent (extended) hemihepatectomy and 46 of these were included in the study. Patients who had a previous PVE (6 patients), combined hepatectomy or radiofrequency ablation (7), synchronous

resection of other organs (6), bile duct reconstruction (2), accompanying macroscopic portal vein tumour thrombus (2) and insufficient perioperative data/diagnostic images (10) were excluded. There were 35 men and 11 women of mean age 65(12) (range 35–84) years; 24 patients had a right-sided hemihepatectomy (6 extended) and 22 a left-sided major hemihepatectomy (8 extended). Primary diagnoses included hepatocellular carcinoma (24), intrahepatic cholangiocarcinoma (8), colorectal liver metastases (8) and other condition (6). Twenty-nine patients were included in group 1 and 17 in group 2. C-tube drainage was avoided because of previous cholecystectomy in five patients, difficulties in insertion in five, no cholecystectomy in one patient and surgeon decision in six patients.

Perioperative findings

Age, sex, liver function, duration of surgery, amount of intraoperative blood loss and frequency of blood transfusion were similar in the two groups (*Table 1*). The estimated total and resected liver volumes were equivalent. According to the new Inuyama classification[12], the extent of liver fibrosis and necroinflammatory activity was similar. Morbidity equal to or greater than grade III, assessed according to the Clavien–Dindo classification[13], was comparable between the groups. Biliary leakage defined as grade III[13] was encountered in one patient in group 1 and one in group 2.

Serum bile acid levels before and after hepatectomy

The median duration of biliary drainage was 10 days (*Table 1*). Mean serum bile acid levels before and on days 1, 3, 7 and 14 after hepatectomy were 12·2(9·9), 3·7(6·7), 2·7(2·1), 5·5(4·0) and 14·1(18·7) μmol/l in group 1, and 9·9(7·6), 2·8(1·6), 11·6(13·5), 17·6(15·0) and 16·7(9·8) μmol/l in group 2 respectively. There was no difference in serum bile acid levels between the two groups before hepatectomy. Serum bile acid levels on days 3 and 7 after hepatectomy were significantly higher in group 2 than in group 1 (*Fig. 1*). Subgroup analysis revealed that serum bile acid levels were similar in the 22 patients who underwent left-sided hepatectomy and the 24 patients who had right-sided hepatectomy. Mean levels on day 3 after hepatectomy in group 1 were 2·8(1·9) and 2·5(2·7) μmol/l for the left- and right-sided groups respectively, and those in group 2 were 12·2(16·0) and 14·3(13·2) μmol/l. These differences had disappeared after cessation of external biliary drainage on day 14 after hepatectomy.

Liver regeneration after hepatectomy

In the 46 patients who underwent hemihepatectomy, liver regeneration volumes on day 7 after surgery were significantly higher in group 2 than in group 1; mean regenerated liver volume was 40·0(158·8) (range from −147 to 226) ml

Table 1 Comparison of perioperative characteristics in 46 patients undergoing major hepatectomy with (group 1) and without (group 2) bile drainage

	Drainage ($n = 29$)	No Drainage ($n = 17$)	P‡
Age (years)*	66(13)	64(11)	0·664
Sex ratio (M : F)	20 : 9	15 : 2	0·139§
$ICGR_{15}$ (%)*	12·7(7·6)	12·2(5·6)	0·833
Child–Pugh grade			1·000§
A	29	17	
B	0	0	
Total bilirubin before hepatectomy (mg/dl)*	0·74(0·29)	0·78(0·18)	0·621
Total liver volume before hepatectomy (ml)*	1294(535)	1390(708)	0·607
Duration of surgery (min)*	431(80)	409(108)	0·441
Intraoperative bleeding (ml)*	503(507)	339(249)	0·221
Blood transfusion	4	0	0·109§
Resected liver weight (g)*	558(404)	624(657)	0·676
F stage†			0·972§
0–2	24	14	
3–4	5	3	
A grade†			0·683§
0–1	17	11	
2–3	12	6	
Complications (Clavien–Dindo grade > III)	5	2	0·618§
Median duration of biliary drainage (days)	10	–	0·002

*Values are mean(s.d.). †The extent of liver fibrosis (F stage) and necroinflammatory activity (A grade) were classified according to the new Inuyama classification[12]. $ICGR_{15}$, indocyanine green retention rate at 15 min. ‡Unpaired t test, except §χ^2 test.

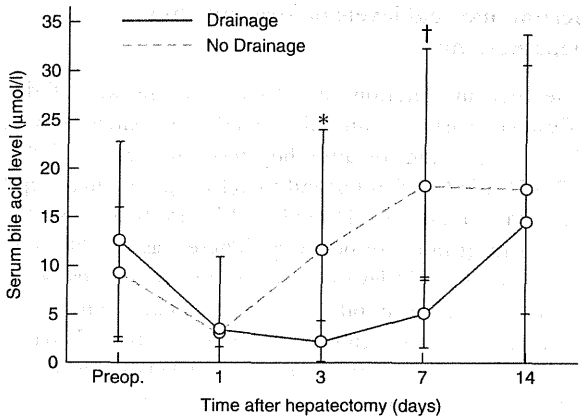

Fig. 1 Changes in mean serum bile acid levels after major hepatectomy in 46 patients undergoing hepatectomy with (group 1) and without (group 2) bile drainage. *$P = 0{\cdot}003$, †$P = 0{\cdot}022$ (unpaired t test)

in group 1 and 138·1(135·9) (−38 to 385) ml in group 2 ($P = 0{\cdot}038$). Mean percentage remnant liver regeneration was 11·0(24·7) (range from −14·1 to 42·3) per cent in group 1 and 22·5(27·6) (−4·3 to 103·5) per cent in group 2 ($P = 0{\cdot}158$). Subgroup analysis of the 22 patients who had a left-sided hemihepatectomy revealed that mean liver regeneration volume on day 7 after surgery was significantly higher in group 2: 149·6(78·6) ml *versus* 24·0(101·5) ml in group 1 ($P = 0{\cdot}018$). In line with this, liver regeneration rates for the remnant liver were significantly higher in group 2 than in group 1 (29·1(16·9) *versus* 3·4(13·1) per cent respectively; $P = 0{\cdot}001$). In the 24 patients who underwent a right-sided hemihepatectomy, mean liver regeneration volumes on day 7 after surgery were significantly higher in group 2 (211·1(140·7) ml *versus* 57·5(149·9) ml in group 1; $P = 0{\cdot}026$). Liver regeneration rates for the remnant liver after right hemihepatectomy were not significantly higher in group 2 (37·6(33·1) *versus* 12·1(25·5) per cent; $P = 0{\cdot}052$).

Association between serum bile acid levels and liver regeneration

The data obtained on day 3 after hepatectomy were selected to predict the extent of liver regeneration as early as possible. Liver regeneration rates on day 7 after hepatectomy showed a significant positive association with serum bile acid levels on day 3 after hepatectomy in the 46 patients included in the study; however, no significant association was observed between regeneration rates on day 7 after hepatectomy and serum bile acid levels on day 1 or 7. Liver regeneration volumes on day 7 after hepatectomy showed a significant positive association with serum bile

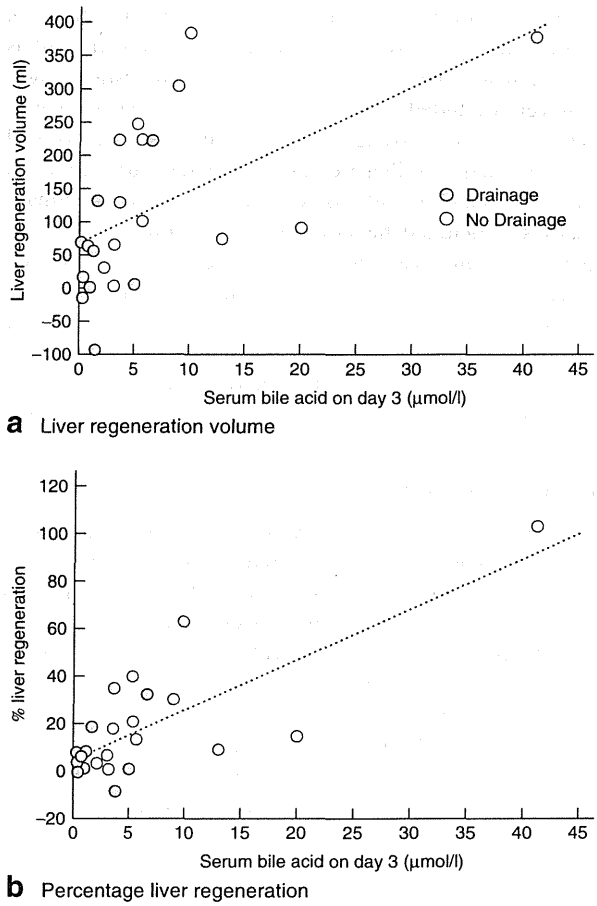

Fig. 2 Association between liver regeneration on day 7 and serum bile acid levels measured on day 3 in patients undergoing major hepatectomy with (group 1, $n = 11$) and without (group 2, $n = 14$) bile drainage: **a** liver regeneration volume; **b** percentage liver regeneration

acid levels on day 3 after hepatectomy. Liver regeneration volumes on day 7 after hepatectomy could be predicted using the formula 68·664 + 7·83× serum bile acid level on day 3 ($R = 0{\cdot}55$, $P = 0{\cdot}006$) (*Fig. 2a*). Similarly, liver regeneration rates on day 7 after hepatectomy showed a significant positive association with serum bile acid levels on day 3 after hepatectomy. Liver regeneration rates on day 7 after hepatectomy were calculated using the equation 4·81 + 2·124 × serum bile acid level on day 3 ($R = 0{\cdot}76$, $P < 0{\cdot}001$) (*Fig. 2b*).

Discussion

In this study, major hepatectomy induced an increase in serum bile acid levels that was more marked among patients

who showed the greatest hypertrophy of the liver. Biliary drainage with a C tube has sometimes been applied to reduce the risk of biliary leakage after hepatectomy[10] and is useful to obtain bile juice for evaluation of liver function[14]. The rate of complications, including biliary leakage, in patients who underwent major hepatectomy with biliary drainage in the present study was similar to that in patients without biliary drainage. In addition, these results clearly demonstrate that external biliary drainage not only caused a significant decrease in serum bile acid levels but also was associated with significantly worse liver regeneration after major hepatectomy. In partially hepatectomized rats, preoperative external biliary drainage leads to loss of bile acid and results in delayed liver regeneration after partial hepatectomy compared with rats with internal biliary drainage[6–8]. The absence of bile acids in the intestine after hepatectomy apparently delays liver regeneration and this may be associated with cyclin E-associated kinase inactivation[8].

In rodent models of 70 per cent partial hepatectomy, bile acid feeding stimulates liver hypertrophy and the rate of liver growth by proliferation of hepatocytes[3]. Bile acids are products of cholesterol catabolism that are synthesized in the liver and secreted into the intestine via the bile duct after food intake. Most of the bile acids are reabsorbed from the intestine and transported back to the liver through the portal vein. External drainage of bile juice at least partially interrupts this enterohepatic circulation. Activation of FXR is required for normal liver regeneration[3]. FXR is a nuclear receptor that recognizes bile acids as endogenous ligands[15]. This receptor plays an important role in mediating crosstalk between the liver and intestine to maintain bile acid, lipid and glucose homeostasis. FXR-knockout mice develop cholestasis, gallstones, non-alcoholic fatty liver disease, carcinogenesis in the liver and systemic metabolic abnormalities[16–19]. The absence of FXR stimulation in the ileum, with less fibroblast growth factor (FGF) 19 production and transport to the liver subsequently, may lead to less hepatic FGF receptor 4 production, which results in increased cytochrome P450 7A1 (CYP7A1) production. Raised levels of CYP7A1 may increase production of bile acids from cholesterol and lead to increased bile acid release into the cholangiocytes[3–5]. As serum concentrations of bile acids were lower in the drained patients, it may be postulated that the extra bile acids produced were drained externally.

Patients who underwent PVE before hepatectomy were excluded from this study. In PVE-treated patients undergoing hepatectomy, liver regeneration follows a two-stage pattern. After PVE, the non-embolized lobe regenerates and subsequently, after major hepatectomy, liver regeneration again occurs but to a lesser extent than that in patients without PVE undergoing a similar liver resection[20]. This study demonstrated that serum bile acid levels on day 3 after hepatectomy were associated with liver regeneration rates and volumes on day 7 after hepatectomy. In support of this, it was previously reported that increases in serum bile acid levels on day 3 after right PVE were strongly associated with effective hypertrophy of the non-embolized liver after PVE[9]. Bile acids are toxic, and increases in hepatic bile acid levels can induce both apoptosis and necrosis of hepatocytes[21]. Bile acid levels in hepatocytes should thus be tightly regulated to prevent cell damage[22] or liver fibrosis[23]. Increased bile acid levels immediately after hepatectomy or PVE may indicate decreased functional capacity of the liver and induce liver regeneration via FXR activation to prevent cell damage. In humans, effective hypertrophy of the remnant liver after hepatectomy and in non-embolized liver after PVE could possibly be evaluated on the basis of serum bile acid levels on day 3. This provides earlier information than increases in transforming growth factor α, serum hepatocyte growth factor and transforming growth factor β1 levels on day 14[24,25].

Disclosure

The authors declare no conflict of interest.

References

1 Buell JF, Rosen S, Yoshida A, Labow D, Limsrichamrern S, Cronin DC *et al.* Hepatic resection: effective treatment for primary and secondary tumors. *Surgery* 2000; **128**: 686–693.

2 Shiratori Y, Shiina S, Imamura M, Kato N, Kanai F, Okudaira T *et al.* Characteristic difference of hepatocellular carcinoma between hepatitis B- and C- viral infection in Japan. *Hepatology* 1995; **22**: 1027–1033.

3 Huang W, Ma K, Zhang J, Qatanani M, Cuvillier J, Liu J *et al.* Nuclear receptor-dependent bile acid signaling is required for normal liver regeneration. *Science* 2006; **312**: 233–236.

4 Xing X, Burgermeister E, Geisler F, Einwächter H, Fan L, Hiber M *et al.* Hematopoietically expressed homeobox is a target gene of farnesoid X receptor in chenodeoxycholic acid-induced liver hypertrophy. *Hepatology* 2009; **49**: 979–988.

5 Zhang L, Huang X, Meng Z, Dong B, Shiah S, Moore DD *et al.* Significance and mechanism of CYP7a1 gene regulation during the acute phase of liver regeneration. *Mol Endocrinol* 2009; **23**: 137–145.

6 Suzuki H, Iyomasa S, Nimura Y, Yoshida S. Internal biliary drainage, unlike external drainage, does not suppress the

regeneration of cholestatic rat liver after partial hepatectomy. *Hepatology* 1994; **20**: 1318–1322.
7 Saiki S, Chijiiwa K, Komura M, Yamaguchi K, Kuroki S, Tanaka M. Preoperative internal biliary drainage is superior to external biliary drainage in liver regeneration and function after hepatectomy in obstructive jaundiced rats. *Ann Surg* 1999; **230**: 655–662.
8 Ueda J, Chijiiwa K, Nakano K, Zhao G, Tanaka M. Lack of intestinal bile results in delayed liver regeneration of normal rat liver after hepatectomy accompanied by impaired cyclin E-associated kinase activity. *Surgery* 2002; **131**: 564–573.
9 Hayashi H, Beppu T, Sugita H, Horino K, Komori H, Masuda T *et al.* Increase in the serum bile acid level predicts the effective hypertrophy of the nonembolized hepatic lobe after right portal vein embolization. *World J Surg* 2009; **33**: 1933–1940.
10 Beppu T, Ishiko T, Chikamoto A, Komori H, Masuda T, Hayashi H *et al.* Liver hanging maneuver decreases blood loss and operative time in a right-side hepatectomy. *Hepatogastroenterology* 2012; **59**: 542–545.
11 Karlo C, Reiner CS, Stolzmann P, Breitenstein S, Marincek B, Weishaupt D *et al.* CT- and MRI-based volumetry of resected liver specimen: comparison to intraoperative volume and weight measurements and calculation of conversion factors. *Eur J Radiol* 2009; **75**: 107–111.
12 Ichida F, Tsuji T, Omata M. New Inuyama Classification; new criteria for histological assessment of chronic hepatitis. *Int Hepatol Commun* 1996; **6**: 112–119.
13 Clavien PA, Barkun J, de Oliveira ML, Vauthey JN, Dindo D, Schulick RD *et al.* The Clavien–Dindo classification of surgical complications: five-year experience. *Ann Surg* 2009; **250**: 187–196.
14 Hotta T, Kobayashi Y, Taniguchi K, Johata K, Sahara M, Ochiai M *et al.* Liver functional analysis by total bile acid level of C-tube bile after hepatectomy. *Hepatogastroenterology* 2005; **52**: 1211–1215.
15 Parks DJ, Blanchard SG, Bledsoe RK, Chandra G, Consler TG, Kliewer SA *et al.* Bile acids: natural ligands for an orphan nuclear receptor. *Science* 1999; **284**: 1365–1368.
16 Moschetta A, Bookout AL, Mangelsdorf DJ. Prevention of cholesterol gallstone disease by FXR agonists in a mouse model. *Nat Med* 2004; **10**: 1352–1358.
17 Guo GL, Santamarina-Fojo S, Akiyama TE, Amar MJA, Paigen BJ, Brewer B Jr *et al.* Effects of FXR in foam-cell formation and atherosclerosis development. *Biochim Biophys Acta* 2006; **1761**: 1401–1409.
18 Yang F, Huang X, Yi T, Yen Y, Moore DD, Huang W. Spontaneous development of liver tumors in the absence of the bile acid receptor farnesoid X receptor. *Cancer Res* 2007; **67**: 863–867.
19 Kong B, Luyendyk JP, Tawfik O, Guo GL. Farnesoid X receptor deficiency induces nonalcoholic steatohepatitis in low-density lipoprotein receptor-knockout mice fed a high-fat diet. *J Pharmacol Exp Ther* 2009; **328**: 116–122.
20 van den Esschert JW, de Graaf W, van Lienden KP, Busch OR, Heger M, van Delden OM *et al.* Volumetric and functional recovery of the remnant liver after major liver resection with prior portal vein embolization: recovery after PVE and liver resection. *J Gastrointest Surg* 2009; **13**: 1464–1469.
21 Kullak-Ublick GA, Meier PJ. Mechanisms of cholestasis. *Clin Liver Dis* 2000; **4**: 357–385.
22 Chiang JY. Bile acid regulation of gene expression: roles of nuclear hormone receptors. *Endocr Rev* 2002; **23**: 443–463.
23 Fiorucci S, Antonelli E, Rizzo G, Renga B, Mencarelli A, Riccardi L *et al.* The nuclear receptor SHP mediates inhibition of hepatic stellate cells by FXR and protects against liver fibrosis. *Gastroenterology* 2004; **127**: 1497–1512.
24 Kusaka K, Imamura H, Tomiya T, Makuuchi M. Factors affecting liver regeneration after right portal vein embolization. *Hepatogastroenterology* 2004; **51**: 532–535.
25 Hayashi H, Beppu T, Sugita H, Masuda T, Okabe H, Takamori H *et al.* Serum HGF and TGF-beta1 levels after right portal vein embolization. *Hepatol Res* 2010; **40**: 311–317.

Surg Today
DOI 10.1007/s00595-012-0371-x

HOW TO DO IT

End-to-side pancreaticojejunostomy without stitches in the pancreatic stump

Daisuke Hashimoto · Masahiko Hirota · Yasushi Yagi · Hideo Baba

Received: 30 March 2012 / Accepted: 5 July 2012

Abstract In patients undergoing pancreaticoduodenectomy, leakage from the pancreatic anastomosis remains an important cause of morbidity and contributes to prolonged hospitalization and mortality. Recently, a new end-to-end pancreaticojejunostomy technique without the use of any stitches through the pancreatic texture or pancreatic duct has been developed. In this novel anastomosis technique, the pancreatic stump is first sunk into deeply and tightened with a purse string in the bowel serosa. We modified this method in an end-to-side manner to complete the insertion of the pancreatic stump into the jejunum, independent of the size of the pancreas or the jejunum. We tested this new anastomosis technique in four pilot patients and compared their outcomes with four control patients who underwent traditional pancreaticojejunostomy. No severe pancreatic fistulas were observed in either group. There were no differences in morbidity or hospital stay between the groups. This new method can be performed safely and is expected to minimize leakage from pancreaticojejunostomies.

Keywords Pancreaticoduodenectomy · Pancreaticojejunostomy · Pancreatic fistula

D. Hashimoto · H. Baba (✉)
Department of Gastroenterological Surgery, Kumamoto University Graduate School of Medical Sciences,
1-1-1 Honjo, Kumamoto 860-8556, Japan
e-mail: hdobaba@kumamoto-u.ac.jp

D. Hashimoto · M. Hirota · Y. Yagi
Department of Surgery, Kumamoto Regional Medical Center,
5-16-10 Honjo, Kumamoto 860-0811, Japan

Introduction

Problems with pancreaticojejunostomies and pancreaticogastrostomy anastomoses are the main causes of early morbidity after pancreaticoduodenectomy (PD) [1–5]. Therefore, this study focused on generating a method for anastomosing the pancreas with the jejunum that might reduce the rate of complications associated with this difficult type of anastomosis.

Recently, it was found that postoperative pancreatic fistula (POPF) may mediate many of the complications observed after pancreatic resection [6]. Several authors have previously reported that a soft pancreatic texture constitutes a major risk factor for postoperative complications, including POPF [7, 8].

The pancreas is extremely vulnerable to handle. The use of surgical scalpels, instead of electrocautery or ultrasonic techniques, may diminish trauma to the pancreatic stump induced by resection [9]. In addition, using a thin suture material with as few stitches as possible and avoiding any excessive tightening of the sutures have been reported to reduce injury to the pancreas in rats [9]. In general, multiple stitches are used to secure the anastomosis between the pancreas and the jejunum or stomach, regardless of the type of reconstruction used. In order to minimize pancreatic injury induced by multiple stitches, a novel anastomosis technique has been developed [10] in which the pancreatic stump is inserted into the jejunum deeply in an end-to-end fashion and tightened with a purse string in the jejunal serosa without the use of any stitches through the pancreatic texture or pancreatic duct [10]. This technique may not be completed if the intestines are too small or the pancreatic stump is too large to insert the pancreatic stump into the jejunum. We modified this method in an end-to-side manner to complete the insertion of the pancreatic stump into the jejunum, independent of the size of the pancreas or the jejunum.

Published online: 11 October 2012

Patients and methods

PD surgical technique

PD was performed with D2 dissection of the lymph nodes [11–13]. There were no patients with possible portal/superior mesenteric vein invasion. In each case, the neck of the pancreas was transected using a surgical scalpel. Artificial bleeding on the side of pancreatic stump was controlled with precisely positioned monofilament sutures, and smaller areas of bleeding were treated with compression. The jejunum was cut, and the cut end of the anal side was moved up retrocolically through the incision in the right side of the transverse mesocolon. Pancreaticojejunostomy was performed in two ways, as described below, and a non-absorbable stent tube was inserted into the main pancreatic duct to avoid obstruction. Hepaticojejunostomy and gastrojejunostomy were performed distal to the pancreaticojejunostomy.

Surgical technique of the new end-to-side pancreaticojejunostomy without stitches in the pancreatic stump

For reconstruction, an incision with the same diameter as the pancreatic stump was made on the opposite side of the mesenterium of the jejunum (Fig. 1a). The pancreatic stump was first isolated from the surrounding tissue with up to a 30-mm margin from the cut surface (Fig. 1b). It is necessary to insert the pancreatic remnant into the jejunum and to maintain a safe fixation between the pancreas and the jejunum. A purse string suture of absorbable 3-0 monofilament thread was applied around the incision of the jejunum (Fig. 1a). Four to five stay sutures of absorbable 4-0 monofilament thread were also applied around the pancreas (Fig. 1b). On the posterior side, stay sutures were applied on the peripancreatic retroperitoneal tissue carefully avoiding stitching the pancreatic parenchyma dissected from the splenic artery and vein, which should be completely covered by the jejunal wall. On the anterior side, stay sutures were applied on the serosa and parenchyma of the pancreas. The pancreatic stump was inserted into the jejunal incision in an end-to-side fashion applying the stay sutures on the incision to secure the depth of insertion (Fig. 1c, d). Finally, the purse string suture was tied to seal the anastomosis carefully avoiding the ischemia of the pancreatic stump. The stay sutures and the purse string sutures prevent the pancreatic stump from dropping out of the jejunum.

Surgical technique of traditional end-to-side pancreaticojejunostomy

Traditional pancreaticojejunostomy was also performed as end-to-side anastomosis. An incision of the jejunal wall proportional to the size of the pancreatic duct was created. Eight to 10 sutures of 4-0 monofilament thread were applied taking the pancreatic duct and the whole pancreatic parenchyma, followed by taking the whole layer of the jejunum, enough to cover the pancreatic stump. After being placed, all sutures were tied.

Patients and POPF

Between 2009 and 2011, eight patients underwent PD at Kumamoto Regional Medical Center. All procedures were performed by one surgeon. Written informed consent was obtained before surgery. Pancreaticojejunostomy was performed using the new method in four pilot patients and using the traditional method in four patients. We evaluated patient backgrounds, operative times, operative bleeding, pancreatic textures and outcomes after surgery. The incidence of POPF was assessed according to the International Study Group (ISGPF) definition [14]. Grade A was excluded from postoperative complications because it had no clinical impact.

Statistical analysis

The median test and the Chi square test were used to evaluate differences in each parameter. A P value < 0.05 was considered to be statistically significant.

Results

The patient characteristics are listed in Table 1. There were no significant differences in age or sex ratios. The pancreatic textures were soft in three of the patients in the new method group and two patients in the traditional method group. The operative parameters and outcomes after surgery are listed in Table 2. There were no significant differences in operative time, bleeding or length of hospital stay after surgery. Delayed gastric empting (DGE) was observed in only one patient in the new method group. Although one patient in the traditional method group developed grade A POPF, there were no hospital deaths or patients with grade B or C POPF in either group.

Discussion

Although PD has been performed safely in high volume centers, mortality and morbidity remain high, and the procedure is largely associated with problems during pancreatic reconstruction [1–4]. In order to minimize surgical damage to the cut end of the pancreas and to cover it completely with the jejunal wall, Nordback et al. [10]

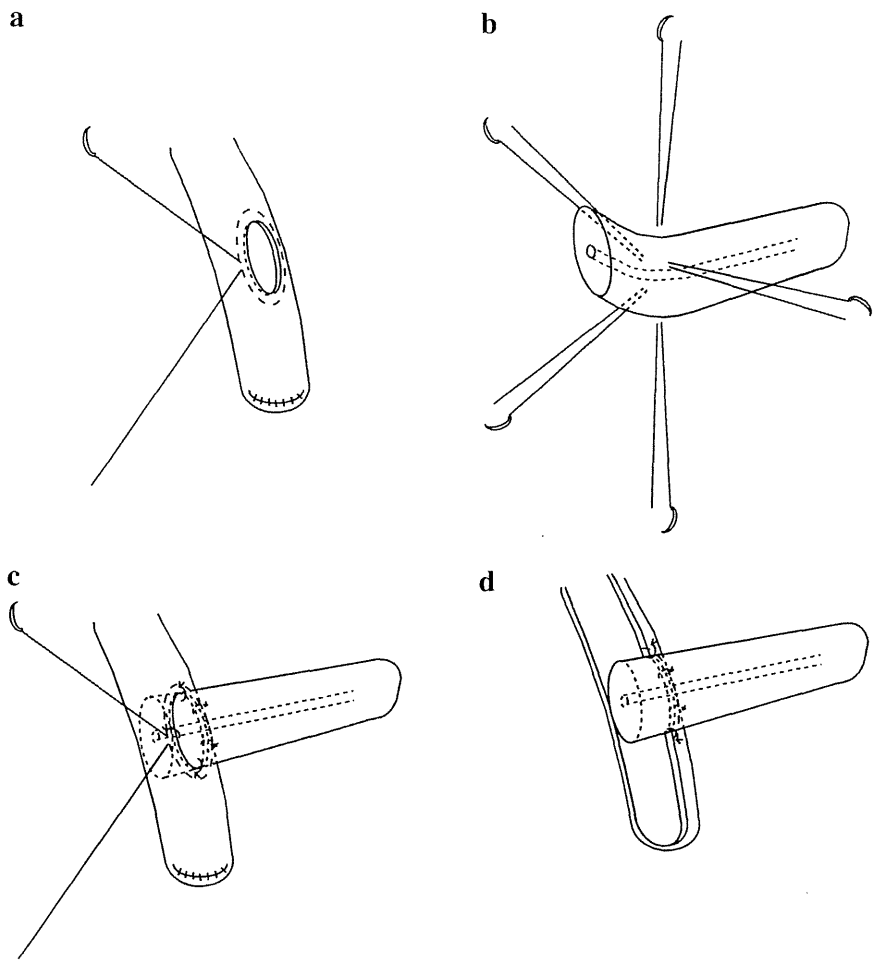

Fig. 1 A schematic drawing of end-to-side pancreaticojejunostomy without stitches in the pancreatic stump. An incision that matches the diameter of the pancreatic stump was made on the opposite side of the mesenterium of the jejunum, and a purse string suture of absorbable 3-0 monofilament thread was applied around the incision of the jejunum (**a**). The pancreatic stump was first isolated from the surrounding tissue with up to a 30-mm margin from the cut surface (**b**). Four to five stay sutures of absorbable 4-0 monofilament thread were also applied around the pancreas (**b**). The pancreatic stump was inserted into the jejunal incision in an end-to-side fashion applying the stay sutures on the incision to secure the depth of insertion (**c**, **d**). Finally, the purse string suture was tied to seal the anastomosis. The pancreatic remnant was sunk into the jejunum without any stitches on the cut end of the pancreas (**d**)

Table 1 Patient characteristics

	New method group	Traditional method group	*P* value
n	4	4	
Age	67 (63–79)	63 (58–68)	0.48
Male:female	3:1	4:0	0.28
Final diagnosis			
Pancreatic cancer	1	2	
Bile duct cancer	1	2	
Vater's papilla cancer	1	0	
Duodenal cancer	1	0	

Table 2 Operative parameters and outcomes after surgery

	New method group	Traditional method group	*P* value
Operating time (min)	420 (293–522)	422 (361–475)	0.48
Operating bleeding (g)	513 (170–890)	745 (210–1040)	0.36
Postoperative complication	1 (DGE)	0	0.28
Hospital stay after surgery (days)	33 (28–37)	32 (29–34)	0.48

DGE delayed gastric empting

developed a new end-to-end pancreaticojejunal anastomosis technique without the use of stitches going through the pancreatic stump. In their end-to-end anastomosis technique, there is a possible problem for a mismatch in the size of the jejunum and the pancreatic remnant. To avoid this problem, we modified Nordback et al.'s anastomosis technique in an end-to-side manner. An incision in the jejunum is made that is the same size as the diameter of the pancreatic remnant. We are not aware of any similar end-to-side pancreaticojejunal anastomosis techniques published in the English literature.

This new end-to-side pancreaticojejunostomy technique did not increase operative times or amounts of bleeding in the four pilot patients. In addition, the patients recovered without developing grade B or C POPF. These results prove that the four patients underwent successful operations,

even those with soft pancreatic textures. It is preferable for surgeons to master conventional techniques before performing this novel technique. This anastomosis technique can be performed safely, independent of the pancreatic texture or the size of the pancreatic duct (and can be used even in patients with a soft pancreas and small pancreatic duct). Additionally, pancreatic juice secreted from the transected pancreatic duct branches faced on the pancreatic stump is drained into the jejunal lumen [10]. Because this is a pilot study to determine whether this new end-to-side anastomosis technique can be performed as designed, further studies including more patients should be conducted to confirm the safety of the technique and whether it significantly decreases the incidence of pancreatic fistulas.

In conclusion, this pilot study showed that it is feasible to create a pancreaticojejunostomy anastomosis without applying any stitches at the cut end of the pancreas or pancreatic duct, independent of the size of the pancreas and the jejunum.

Conflict to interest No authors have any conflicts to interest.

References

1. Fernández-Cruz L, Belli A, Acosta M, Chavarria EJ, Adelsdorfer W, López-Boado MA, et al. Which is the best technique for pancreaticoenteric reconstruction after pancreaticoduodenectomy? A critical analysis. Surg Today. 2011;41:761–6.
2. Kawai M, Yamaue H. Analysis of clinical trials evaluating complications after pancreaticoduodenectomy: a new era of pancreatic surgery. Surg Today. 2010;40:1011–7.
3. Hirota M. Percutaneous transfistulous interventions for intractable pancreatic fistula. Radiol Res Pract. 2011;2011:109259.
4. Hirota M, Kanemitsu K, Takamori H, Chikamoto A, Hayashi N, Horino K, et al. Percutaneous transfistulous pancreatic duct drainage and interventional pancreatojejunostomy as a treatment option for intractable pancreatic fistula. Am J Surg. 2008;196:280–4.
5. Hashimoto D, Takamori H, Sakamoto Y, Ikuta Y, Nakahara O, Furuhashi S, et al. Is an estimation of physiologic ability and surgical stress able to predict operative morbidity after pancreaticoduodenectomy? J Hepatobiliary Pancreat Sci. 2010;17:132–8.
6. Räty S, Sand J, Lantto E, Nordback I. Postoperative acute pancreatitis as a major determinant of postoperative delayed gastric emptying after pancreaticoduodenectomy. J Gastrointest Surg. 2006;10:1131–9.
7. Suzuki Y, Fujino Y, Tanioka Y, Hiraoka K, Takada M, Ajiki T et al. Selection of pancreaticojejunostomy techniques according to pancreatic texture and duct size. Arch Surg 2002;137:1044–7 (discussion 1).
8. Yang YM, Tian XD, Zhuang Y, Wang WM, Wan YL, Huang YT. Risk factors of pancreatic leakage after pancreaticoduodenectomy. World J Gastroenterol. 2005;11:2456–61.
9. Lämsä T, Jin HT, Nordback PH, Sand J, Luukkaala T, Nordback I. Pancreatic injury response is different depending on the method of resecting the parenchyma. J Surg Res. 2009;154:203–11.
10. Nordback I, Lämsä T, Laukkarinen J, Leppiniemi J, Kellomäki M, Sand J. Pancreatico-jejunostomy with a biodegradable pancreatic stent and without stitches through the pancreas. Hepatogastroenterol. 2008;55:319–22.
11. Japan Pancreas Society. General rules for the study of pancreatic cancer, 6th edn. 2009.
12. Japanese society of biliary surgery. Society general rules for surgical and pathological studies on cancer of the biliary tract, 5th edn. 2003.
13. Hirota M, Kanemitsu K, Takamori H, Chikamoto A, Tanaka H, Sugita H, et al. Pancreatoduodenectomy using a no-touch isolation technique. Am J Surg. 2010;199:e65–8.
14. Bassi C, Dervenis C, Butturini G, Fingerhut A, Yeo C, Izbicki J, et al. Postoperative pancreatic fistula: an international study group (ISGPF) definition. Surgery. 2005;138:8–13.

LINE-1 Hypomethylation Is Associated With a Poor Prognosis Among Patients With Curatively Resected Esophageal Squamous Cell Carcinoma

Shiro Iwagami, MD, Yoshifumi Baba, MD, PhD,* Masayuki Watanabe, MD, PhD, FACS,* Hironobu Shigaki, MD,* Keisuke Miyake, MSc,* Takatsugu Ishimoto, MD, PhD,* Masaaki Iwatsuki, MD, PhD,* Kentaro Sakamaki, MPH,† Yasuo Ohashi, PhD,† and Hideo Baba, MD, PhD, FACS**

Objective: To investigate the relationship between the long interspersed nucleotide element-1 (L1/LINE-1) methylation level and the disease-free survival and cancer-specific survival in patients with esophageal squamous cell carcinoma (ESCC).

Background: Cancer cells exhibit 2 types of deoxyribonucleic acid (DNA) methylation alterations: global DNA hypomethylation and site-specific CpG island promoter hypermethylation. Global DNA hypomethylation plays a role in genomic instability and carcinogenesis. DNA methylation in the LINE-1 repetitive element is a good indicator of the global DNA methylation level. Although the LINE-1 methylation level is attracting interest as a useful marker for predicting cancer prognosis, the prognostic significance of LINE-1 hypomethylaiton in ESCC remains unclear.

Methods: Using 217 curatively resected ESCC specimens, we quantified the LINE-1 methylation by utilizing the bisulfite pyrosequencing technology. Promoter methylation levels of *MGMT* and *MLH1* were also evaluated by pyrosequencing.

Results: ESCC showed significantly lower LINE-1 methylation levels in comparison with matched normal esophageal mucosa ($P < 0.0001$; N = 50). LINE-1 hypomethylation was significantly associated with disease-free survival [log-rank $P = 0.0008$; univariate hazard ratio (HR): 2.32, 95% confidence interval (CI): 1.38–3.84, $P = 0.0017$; multivariate HR: 1.81, 95% CI: 1.06–3.05, $P = 0.031$] and cancer-specific survival (log-rank $P = 0.0020$; univariate HR: 2.21, 95% CI: 1.33–3.60, $P = 0.0026$; multivariate HR: 1.87, 95% CI: 1.12–3.08, $P = 0.018$]. *MGMT* and *MLH1* hypermethylation were not associated with patient prognosis.

Conclusions: LINE-1 hypomethylation in ESCC is associated with a shorter survival, thus suggesting that it has potential for use as a prognostic biomarker.

Keywords: epigenetics, esophageal cancer, LINE-1, methylation, prognosis, pyrosequencing

(*Ann Surg* 2013;257: 449–455)

Esophageal squamous cell carcinoma (ESCC), the major histological type of esophageal cancer in east Asian countries, is one of the most aggressive malignant tumors.[1] Despite the development of multimodality therapies, the prognosis of patients remains poor, even for those who undergo complete resection of their carcinomas.[2–4] The limited improvements in treatment outcomes provided by conventional therapies have prompted us to seek innovative strategies for treating ESCC, especially those that are molecularly targeted. Importantly, epigenetic changes, including alterations in deoxyribonucleic acid (DNA) methylation, are reversible, and can thus be targets for therapy or chemoprevention.[5–7] In addition, the identification of new prognostic or predictive molecular markers for ESCC could improve the risk-adapted treatment strategies and help stratify patients in future clinical trials for drugs targeting these molecular changes.[8,9]

DNA methylation is a major epigenetic mechanism involved in X-chromosome inactivation, imprinting, and the repression of endogenous retroviruses.[5–7] DNA methylation alterations associated with human cancers include global DNA hypomethylation and site-specific CpG island promoter hypermethylation. Promoter hypermethylation can silence tumor suppressor genes, DNA mismatch repair genes (eg, *MLH1*), or DNA repair genes (eg, *MGMT*), thereby contributing to esophageal carcinogenesis.[10] Global DNA hypomethylation appears to play an important role in genomic instability, leading to cancer development.[11–13] As long interspersed nucleotide element-1 (LINE-1 or L1) retrotransposon constitutes a substantial portion (approximately 17%) of the human genome, the level of LINE-1 methylation is regarded to be a surrogate marker of global DNA methylation.[14] Measurement of LINE-1 methylation by pyrosequencing technology has emerged as a cost-effective and high-throughput method to assess the global DNA methylation status.[15–17] In several types of human neoplasms, LINE-1 methylation has been shown to be highly variable, and LINE-1 hypomethylation is strongly associated with a poor prognosis.[18–20] However, the influence of LINE-1 hypomethylation on the prognosis of ESCC patients remains unclear.

In this study, we quantified the LINE-1 methylation in 217 samples of curatively resected ESCCs by utilizing a bisulfite–polymerase chain reaction (PCR)–pyrosequencing assay, and examined prognostic significance of LINE-1 hypomethylation in ESCC. In addition, the promoter hypermethylation of *MGMT* and *MLH1* was also evaluated in association with patient survival. Our data suggest that LINE-1 hypomethylation can have a potential role as a prognostic biomarker.

METHODS

Study Subjects

A total of 231 consecutive patients with ESCC who were undergoing curative resection at Kumamoto University Hospital (Kumamoto, Japan) between April 2005 and December 2010 were enrolled in this study. Nine patients were excluded due to the unavailability of adequate tissue samples. We initially quantified LINE-1 methylation in 222 cancer specimens, and obtained valid results in 217 (98%) of the cases. Thus, a total of 217 ESCCs were finally included in this study. Patients were observed at 1 to 3-month

From the *Department of Gastroenterological Surgery, Graduate School of Medical Science, Kumamoto University, Kumamoto, Japan; and †Department of Biostatistics, School of Public Health, University of Tokyo, Tokyo, Japan.

S. Iwagami and Y. Baba contributed equally.

Disclosure: This work was supported in part by the Japan Society for the Promotion of Science (JSPS) Grant-in-Aid for Scientific Research, grant number 23689061 and the Kobayashi Foundation for Cancer Research. No conflict of interest exists.

Supplemental digital content is available for this article. Direct URL citations appear in the printed text and are provided in the HTML and PDF versions of this article on the journal's Web site (www.annalsofsurgery.com).

Reprints: Hideo Baba, MD, PhD, FACS, Department of Gastroenterological Surgery, Graduate School of Medical Science, Kumamoto University, 1–1–1 Honjo, Kumamoto City, Kumamoto 860–8556, Japan. E-mail: hdobaba@kumamoto-u.ac.jp.

ISSN: 0003-4932/13/25703-0449
DOI: 10.1097/SLA.0b013e31826d8602

intervals until death or June 30, 2011, whichever came first. Tumor staging was done by the American Joint Committee on Cancer's *Cancer Staging Manual* (7th edition).[21] Sixty-nine patients received preoperative treatment {41 patients: chemotherapy [cisplatin, 5-fluorouracil either with or without docetaxel], 4 patients: radiation therapy, 24 patients: chemoradiotherapy}. Disease-free survival was defined as the length of time after surgical treatment for the cancer during which the patient survived with no sign of cancer recurrence. Overall survival was defined as the time between the date of the operation and the date of death. Cancer-specific survival was defined as the time between the date of operation and the date of death that was confirmed to be attributable to ESCC. Written informed consent was obtained from each subject, and the study procedures were approved by the Institutional Review Board. The term "prognostic marker" is used throughout this paper according to the REMARK Guidelines.[22]

DNA Extraction and Sodium Bisulfite Treatment

Hematoxylin and eosin-stained slides of the tumors were reviewed by 1 pathologist, who marked the areas of the tumor and normal mucosa. Hematoxylin and eosin-stained tissue sections (depending on tissue and tumor size: on average, large tumor tissue 10 μm × 1 section) from each case were scraped off slides for DNA extraction. Genomic DNA extraction from the tumor and normal mucosa, and sodium bisulfite treatment on genomic DNA were performed as previously described by Ogino et al.[18,23–25]

Pyrosequencing to Measure LINE-1 Methylation

Polymerase chain reaction and subsequent pyrosequencing for LINE-1 were performed as previously described by Ogino et al, using the PyroMark kit (Qiagen).[18,23,24] This assay amplifies a region of LINE-1 element (position 305–331 in accession no. X58075), which includes 4 CpG cites. The PCR conditions were 45 cycles of 95°C for 20 seconds, 50°C for 20 seconds, and 72°C for 20 seconds, followed by 72°C for 5 minutes. The biotinylated PCR product was purified and made single-stranded to act as a template in a pyrosequencing reaction, using the Pyrosequencing Vacuum Prep Tool (Qiagen). Pyrosequencing reactions were performed in the PyroMark Q24 System (Qiagen). The nucleotide dispensation order was: ACT CAG TGT GTC AGT CAG TTA GTC TG. The non-CpG cytosine in LINE-1 repetitive sequences has been documented to be rarely methylated. Thus, complete conversion of cytosine at a non-CpG site ensured successful bisulfite conversion. The amount of C relative to the sum of the amounts of C and T at each CpG site was calculated as the percentage (ie, 0 to 100). The average of the relative amounts of C in the 4 CpG sites was used as the overall LINE-1 methylation level in a given tumor (Fig. 1).

Pyrosequencing to Measure Promoter Methylation of *MGMT* and *MLH1*

Pyrosequencing for *MGMT* and *MLH1* was performed using the PyroMark kit (Qiagen). We used the previously defined cutoff of ≥8% methylated alleles for *MGMT* and *MLH1* hypermethylated tumors.[26]

Statistical Methods

For the statistical analyses, we used the JMP (Version 9, SAS Institute, Cary, NC) and the SAS software programs (Version 9.1, SAS Institute, Cary, NC). All *P*-values were 2-sided. To compare the means, we performed the *t* test assuming unequal variances. For the survival analysis, the Kaplan-Meier method was used to assess the survival time distribution, and the log-rank test was used. To assess the independent effect of the LINE-1 methylation level on mortality, the tumor stage (IA + IB, IIA + IIB, IIIA + IIIB + IIIC) was used as a stratifying (matching) variable in Cox models using the "strata" option in the SAS "proc phreg" command to avoid residual confounding and overfitting. We constructed a multivariate, stage-stratified Cox proportional hazard model to compute a hazard ratio (HR) according to LINE-1 methylation status, containing sex (male vs female), age at surgery (continuous variable), tobacco use (yes vs no), alcohol use (yes vs no), year of diagnosis (2005–2007 vs 2008–2010), preoperative treatment (present vs absent), and histological grade (G1 vs G2–4). A backward stepwise elimination with a threshold of $P = 0.20$ was used to select variables in the final model. For cases with missing information in any of the categorical variables [tobacco use (5.1%) and alcohol use (6.9%)], we used a complete-subject method for model selection and final model. After the selection was done, we assigned separate missing indicator variables to those cases with missing information in the final model. An interaction was assessed by including the cross product of the LINE-1 variable and another variable of interest (without data-missing cases) in a multivariate Cox model, and thereafter the Wald test was performed. To validate the cutoff value, the *C* statistics for survival data established by Uno et al was estimated, which is similar to time-dependent receiver operating characteristic curve analysis.[27] The "survivalROC" package in

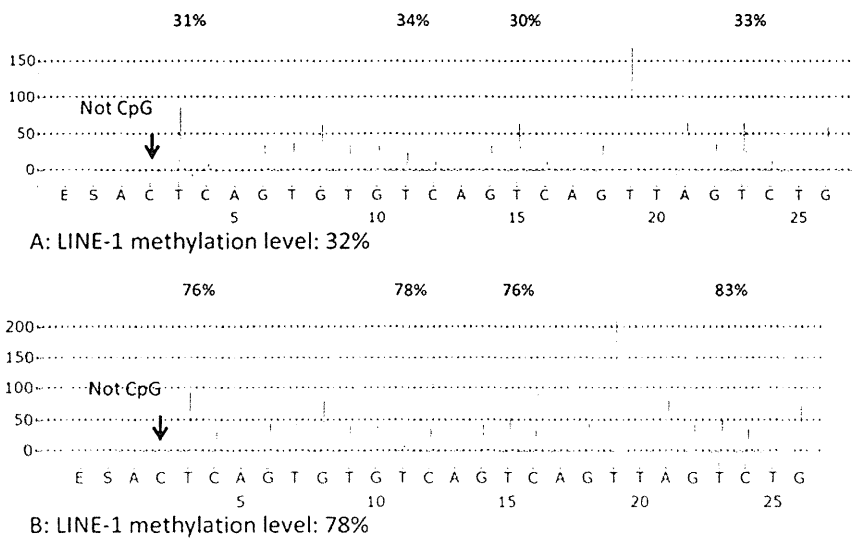

FIGURE 1. The pyrosequencing assay used to measure the LINE-1 methylation level. A, A LINE-1 hypomethylated tumor (methylation level, 32). B, A LINE-1 hypermethylated tumor (methylation level, 78). The percentages (in blue) are the proportion of C at each CpG site after bisulfite conversion, and the methylation level of each CpG site was estimated by the proportion of C (%). The overall LINE-1 methylation level was calculated as the average of the proportions of C (%) at the 4 CpG sites. The first, third, and fourth CpG sites follow mononucleotide T repeats, resulting in higher T peaks than in the case of the second CpG site, and the proportion of C (%) has been adjusted accordingly. The arrows indicate no residual C at the non-CpG site, ensuring complete bisulfite conversion.

the open-source statistical software R (http://www.R-project.org) was used for the analysis.

RESULTS

LINE-1 Methylation in Esophageal Squamous Cell Carcinoma and Matched Normal Mucosa

We first examined the LINE-1 methylation level in 50 ESCC tissues and matched normal esophageal mucosa samples. The cancer tissues exhibited significantly lower levels of LINE-1 methylation [median, 65.1; mean, 63.3; standard deviation, 12.7 (all in 0–100 scale)] than the matched normal mucosa (median, 79.3; mean, 78.8; standard deviation, 6.2) ($P < 0.0001$ by the paired t test) (Fig. 2A).

Evaluation of Association of LINE-1 Methylation Level and Clinical, Epidemiological, and Pathological Variables

Next, we quantified the LINE-1 methylation in 222 cancer specimens, and obtained valid results in 217 (98%) of cases. The distribution of the LINE-1 methylation level in the 217 cancers (Fig. 2B) was as follows: mean, 64.5; median, 65.0; standard deviation, 12.8; range, 24.8 to 91.8; interquartile range, 55.5 to 74.5 (all in 0–100 scale). The LINE-1 methylation level was then divided into quartiles [Q1 (≥74.6, n = 54), Q2 (65.0–74.5, n = 55), Q3 (55.5–64.9, n = 54), and Q4 (<55.5, n = 54)] for further analyses. However, we found that the LINE-1 methylation level was not associated with any of the clinical, epidemiological, or pathological characteristics (all $P > 0.18$, Table 1).

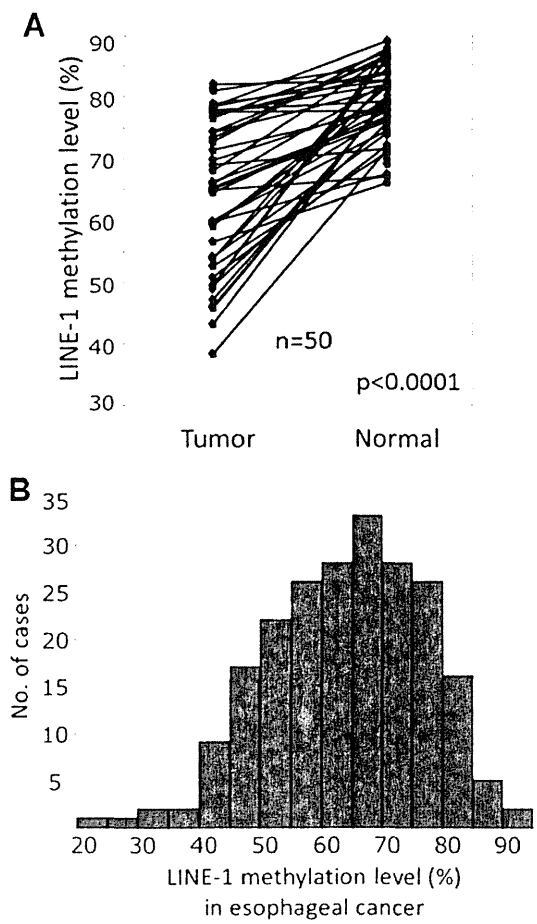

FIGURE 2. The LINE-1 methylation levels in esophageal cancer. A, The LINE-1 methylation levels in 50 esophageal cancer and matched normal mucosa specimens. The cancer tissues showed significantly lower levels of methylation than the matched normal mucosa ($P < 0.0001$ by the paired t test). B, The distribution of the LINE-1 methylation levels in 217 esophageal cancers.

LINE-1 Hypomethylation and Patient Survival

During the follow-up of the 217 patients, there were a total of 63 esophageal cancer recurrences and 51 deaths that were confirmed to be attributable to esophageal cancer. The median follow-up time for censored patients was 2.6 years.

We performed the Cox regression analysis with LINE-1 methylation as a continuous variable. LINE-1 hypomethylation was associated with a statistically significant increase in disease recurrence (univariate analysis $P < 0.001$) and cancer-specific mortality (univariate analysis $P < 0.001$). The univariate HR for disease recurrence rate associated with a 20% decrease in LINE-1 methylation was 2.23 (95% confidence interval [CI]: 1.50–3.32), whereas that of the cancer-specific mortality was 2.39 (95% CI: 1.54–3.70).

We performed the Cox regression analysis using a categorical variable [ie, the first quartile cases (Q1), the second quartile cases (Q2), the third quartile cases (Q3), and the fourth quartile cases (Q4)]. In a univariate Cox regression analysis, compared with Q1 cases, Q4 cases experienced a significantly higher disease recurrence rate [$P = 0.0020$, HR: 3.39; 95% CI: 1.64–7.70], whereas Q2 and Q3 cases experienced a slightly, but not significantly, higher disease recurrence rate compared with Q1 cases ($P = 0.12$ for Q2 and $P = 0.46$ for Q3) (Table 2). Similar results were observed in the multivariate analysis for disease-free survival (Table 2), in the univariate and multivariate analyses for cancer-specific survival (Table 2), and in the univariate and multivariate analyses for overall survival (data not shown). Thus, we made a dichotomous LINE-1 methylation variable, defining Q4 as the "hypomethylated group" and combining Q1, Q2, and Q3 into the "hypermethylated group."

In the Kaplan-Meier analysis, LINE-1 hypomethylators (ie, Q4 cases) experienced significantly shorter disease-free survival (log-rank $P = 0.0008$) and cancer-specific survival (log-rank $P = 0.0020$) than those with hypermethylation (Fig. 3). In the univariate Cox regression analysis, compared with LINE-1 hypermethylated cases, LINE-1 hypomethylated cases experienced a significantly higher disease recurrence rate (HR: 2.32; 95% CI: 1.38–3.84; $P = 0.0017$] (Table 2). In the multivariate Cox model adjusted for the clinical, pathological, and epidemiological features, LINE-1 hypomethylation was found to be associated with a significantly higher disease recurrence rate (multivariate HR: 1.81; 95% CI: 1.06–3.05; $P = 0.031$). Similar results were observed in an analysis of the cancer-specific mortality (Table 2) and overall mortality (data not shown).

The C statistics for survival data were also estimated to validate the cutoff value of LINE-1 hypomethylation. We generated a Cox regression model with LINE-1 methylation level and obtained the estimated C statistics, as the cutoff value of LINE-1 "hypomethylation," "<30," "<40," "<50," "<60," "<70," or "<80," has been tested. The estimated risk score was highest (0.71) in the case where LINE-1 hypomethylation was defined as "<50." This result may support the validity of our cutoff value (ie, <55.5).

Interaction Between LINE-1 Hypomethylation and Other Variables in Survival Analyses

We also examined whether the influence of LINE-1 hypomethylation on the disease-free survival was modified by any of

TABLE 1. LINE-1 Methylation in Esophageal Cancer Specimens and Association with Clinical and Tumor Features

Clinical, Epidemiological, or Pathological Feature	Total N	LINE-1 Methylation (Quartile)				P
		Q1 (≥74.6)	Q2 (65.0–74.5)	Q3 (55.5–64.9)	Q4 (<55.5)	
All cases	217	54	55	54	54	
Mean age ± standard deviation	65.9 ± 9.1	66.3 ± 8.6	66.8 ± 9.1	65.1 ± 8.4	65.6 ± 10.5	0.78
Sex						0.44
Male	192 (88%)	45 (83%)	50 (91%)	47 (87%)	50 (93%)	
Female	25 (12%)	9 (17%)	5 (9.1%)	7 (13%)	4 (7.4%)	
Tobacco use						0.81
Yes	164 (80%)	34 (76%)	45 (83%)	42 (79%)	43 (81%)	
No	41 (20%)	11 (24%)	9 (17%)	11 (21%)	10 (19%)	
Alcohol use						0.60
Yes	171 (87%)	34 (81%)	46 (90%)	44 (88%)	47 (88%)	
No	25 (13%)	8 (19%)	5 (9.8%)	6 (12%)	6 (12%)	
Year of diagnosis						0.33
2005–2007	86 (40%)	19 (35%)	19 (35%)	27 (50%)	21 (39%)	
2008–2010	131 (60%)	35 (65%)	36 (65%)	27 (50%)	33 (41%)	
Preoperative treatment						0.33
Present	69 (32%)	18 (33%)	14 (25%)	15 (28%)	22 (41%)	
Absent	148 (68%)	36 (67%)	41 (75%)	39 (72%)	32 (59%)	
Stage						0.51
I (IA, IB)	99 (46%)	27 (50%)	29 (53%)	20 (37%)	23 (43%)	
II (IIA, IIB)	47 (22%)	11 (20%)	13 (24%)	11 (20%)	12 (22%)	
III (IIIA, IIIB, IIIC)	71 (33%)	16 (30%)	13 (24%)	23 (43%)	19 (35%)	
Lymph node metastasis						0.18
Positive	96 (44%)	21 (39%)	20 (36%)	30 (56%)	25 (46%)	
Negative	121 (56%)	33 (61%)	35 (64%)	24 (44%)	29 (54%)	
Histological grade						0.55
G1	90 (41%)	26 (48%)	22 (40%)	25 (46%)	17 (31%)	
G2	92 (42%)	22 (41%)	22 (40%)	21 (39%)	27 (50%)	
G3–4	35 (16%)	6 (11%)	11 (20%)	8 (15%)	10 (19%)	

Percentage (%) indicates the proportion of cases with a specific clinical, pathological, or epidemiological feature among each quartile group (Q1, Q2, Q3, or Q4).

TABLE 2. Association of LINE-1 Methylation Status in Esophageal Cancer With Patient Mortality

LINE-1 Methylation Level (Quartile)	Total N	Disease-Free Survival			Cancer-Specific Survival		
		Univariate HR (95% CI)	Stage-matched HR (95% CI)	Multivariate stage-matched HR (95% CI)	Univariate HR (95% CI)	Stage-matched HR (95% CI)	Multivariate stage-matched HR (95% CI)
Q1 (≥74.6)	54	1 (referent)	1 (referent)	1 (referent)	1 (referent)	1 (referent)	1 (referent)
Q2 (65.0–74.5)	55	1.92 (0.87–4.54)	1.98 (0.89–4.68)	1.83 (0.80–4.46)	1.77 (0.82–4.05)	1.73 (0.79–3.94)	1.76 (0.80–4.09)
Q3 (55.5–64.9)	54	1.45 (0.64–3.60)	1.30 (0.56–3.15)	1.25 (0.52–3.13)	1.39 (0.62–3.23)	1.26 (0.56–2.94)	1.24 (0.54–2.95)
Q4 (<55.5)	54	3.39 (1.64–7.70)	2.86 (1.38–6.52)	2.50 (1.16–5.86)	3.04 (1.51–6.62)	2.72 (1.35–5.93)	2.47 (1.20–5.48)
P for trend		0.0062	0.019	0.072	0.011	0.024	0.055
Q1–3 (≥55.5)	163	1 (referent)	1 (referent)	1 (referent)	1 (referent)	1 (referent)	1 (referent)
Q4 (<55.5)	54	2.32 (1.38–3.84)	2.04 (1.21–3.38)	1.81 (1.06–3.05)	2.21 (1.33–3.60)	2.06 (1.24–3.37)	1.87 (1.12–3.08)
P		0.0017	0.0079	0.031	0.0026	0.0060	0.018

the clinical, pathological, and epidemiological variables. We found a significant modifying effect of the tumor stage on the relationship between LINE-1 methylation and the recurrence rate (P for interaction = 0.031; Fig. 4), although this could be a chance event considering multiple hypothesis testing. Among the patients with stage I tumors, LINE-1 hypomethylated cases experienced a significantly shorter disease-free survival (log-rank $P = 0.0006$; Fig. 5). In contrast, among patients with stage II and III tumors, the effect of LINE-1 hypomethylation on disease-free survival was slightly attenuated (log-rank, $P = 0.11$; Fig. 5). Similar results were obtained when cancer-specific mortality was used as the endpoint (data not shown). We did not observe a significant interaction with LINE-1 hypomethylation in the survival analysis for any other variables (all P for interactions > 0.12; Fig. 4).

Analyses Excluding Patients With Preoperative Therapy

The effect of preoperative chemotherapy and/or radiotherapy on LINE-1 methylation level is not known. Therefore, we also performed additional analyses excluding ESCC patients who had received preoperative therapy. The distribution of LINE-1 methylation level in 148 patients without preoperative therapy was very similar to that in 217 patients with or without preoperative therapy: mean,